

We are IntechOpen, the world's leading publisher of Open Access books Built by scientists, for scientists

6,900

Open access books available

186,000

International authors and editors

200M

Downloads

Our authors are among the

154

Countries delivered to

TOP 1%

most cited scientists

12.2%

Contributors from top 500 universities



WEB OF SCIENCE™

Selection of our books indexed in the Book Citation Index
in Web of Science™ Core Collection (BKCI)

Interested in publishing with us?
Contact book.department@intechopen.com

Numbers displayed above are based on latest data collected.
For more information visit www.intechopen.com



Arsenomolybdates for Photocatalytic Degradation of Organic Dyes

Zhi-Feng Zhao

Abstract

Polyoxometalates (POMs) have fascinating structures and promising properties. The arsenomolybdates, as an important branch of POMs, are outstanding photocatalysts for organic dyes. In this work, we selected organic dyes to evaluate the photocatalytic activity of arsenomolybdates under UV light, containing compared with photocatalytic activity of different structural arsenomolybdates, stability, and the photocatalytic reaction mechanism of arsenomolybdates as photocatalyst. The arsenomolybdates may be used to as environmental photocatalysts for the degrading of organic dyes and solving the problem of environmental pollution.

Keywords: arsenomolybdates, photocatalyst, photocatalytic activity, organic dyes, UV light

1. Introduction

POMs is one of the most outstanding materials in modern chemistry, as the metal-oxide clusters with abundant structures and interesting properties [1–6], which render them to potential applications in electrochemistry [7, 8], photochemistry [9, 10], catalytic fields [11, 12], and so on (**Figure 1**). Chalkley reported the photoredox conversion of $\text{H}_3[\text{PW}_{12}\text{O}_{40}]$ into a reduced POM by photoirradiation with UV light in the presence of 2-propanol as a reducing reagent in 1952 [13]. Hill et al. started systematic investigation of photoredox catalysis using POMs in the 1980s [14]. Accordingly, POMs photocatalysis has been applied to a wide range of reactions, including H_2 evolution, O_2 evolution, CO_2 reduction, metal reduction, and the degradation of organic pollutants and dyes [15–20].

POMs are subdivided into isopolyoxometalates, which feature addenda metal and oxygen atoms, and heteropolyoxometalates, where a central heteroatom provides added structural stabilization and enables reactivity tuning [21]. In recent years, the research of POMs is mainly focused on heteropolyoxometalates. The arsenomolybdates are essential member of the heteropolymolybdates family [22], because of the redox properties of Mo and As atoms. The discoveries of many excellent articles on arsenomolybdates for ferromagnetic, antitumor activity, electrocatalysis properties, and lithium-ion battery performance have been reported in the last years [23–26]. However, there is no stress and discuss on the progress of arsenomolybdates for degradation of organic dyes. Arsenomolybdates possess

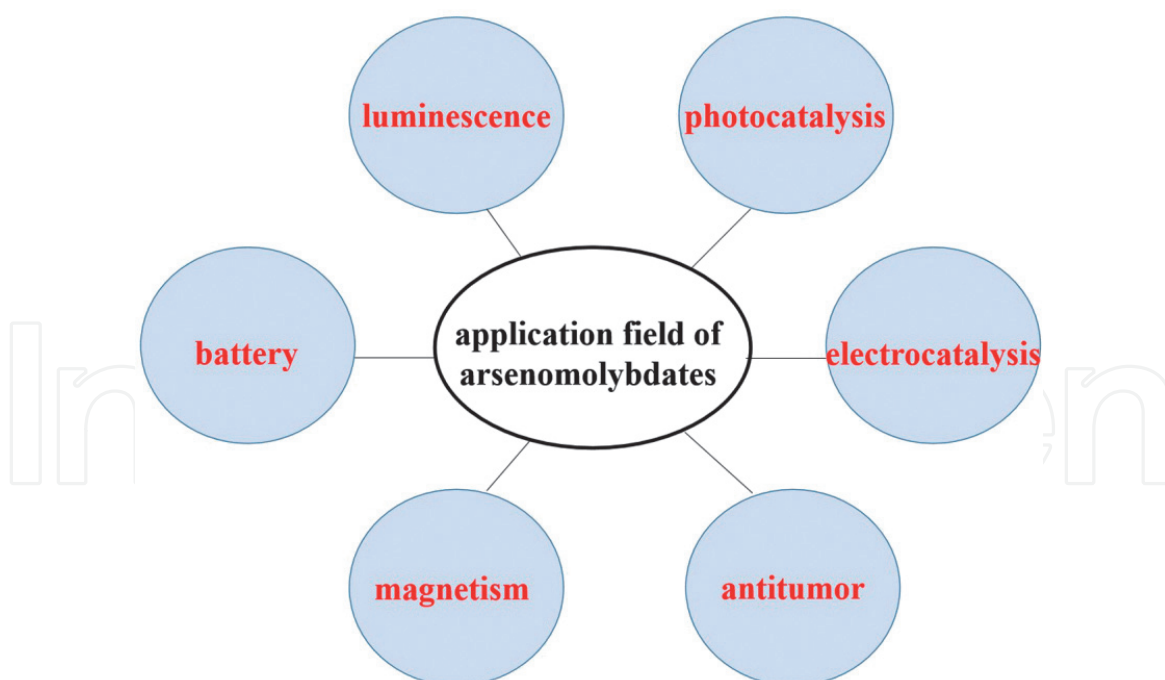


Figure 1.
The potential application field of arsenomolybdates.

high-efficient proton delivery, fast multi-electron transfer, strong solid acidity and excellent reversible redox activity [27], which may result to prominent photocatalytic activities. In particular, the integration of metal-organic frameworks (MOFs) into arsenomolybdates for photocatalysis has attracted widespread attention over the past decade, since MOFs combine porous structural and ultrahigh internal surface areas.

Based on these results, we provide a summary of recent works in the synthesis, structure, the photocatalytic activity, reaction kinetics and mechanism mechanisms of arsenomolybdates, which aim at finding the direction followed with the opportunities and challenges for the arsenomolybdates photocatalysis to accelerate the step to realize its practical application in degradation of organic dyes.

2. Syntheses and structure of arsenomolybdates

2.1 Syntheses of arsenomolybdates

Arsenomolybdates crystals reported were almost synthesized via self-assembly processes using hydrothermal method (**Figure 2**). Many factors in the synthetic process should be considered, such as reaction time and temperature, concentration of starting materials, compactness, pH values, and so on. The some experiments indicate that the temperatures are in the range of 110–180°C for srseptomolybdates synthesized, when the pH value of the mixture is adjusted to approximately 3–6.8, $[\text{H}_x\text{As}_2\text{Mo}_6\text{O}_{26}]^{(6-x)-}$ (abbreviated $\{\text{As}_2\text{Mo}_6\}$), $[(\text{MO}_6)(\text{As}_3\text{O}_3)_2\text{Mo}_6\text{O}_{18}]^{4-}$ (abbreviated $\{\text{As}_6\text{Mo}_6\}$) and $[\text{As}^{\text{III}}\text{As}^{\text{V}}\text{Mo}_9\text{O}_{34}]^{6-}$ (abbreviated $\{\text{As}_2\text{Mo}_9\}$) types were easy to formed, when the pH value is within the range of 2.5–5.5 and 2–4, $[\text{AsMo}_{12}\text{O}_{40}]^{3-}$ (abbreviated $\{\text{AsMo}_{12}\}$) and $[\text{As}_2\text{Mo}_{18}\text{O}_{62}]^{6-}$ (abbreviated $\{\text{As}_2\text{Mo}_{18}\}$) types were successfully synthesized. At the same time, the choice of transition metal, organic ligand, and molybdenic source have also affect for

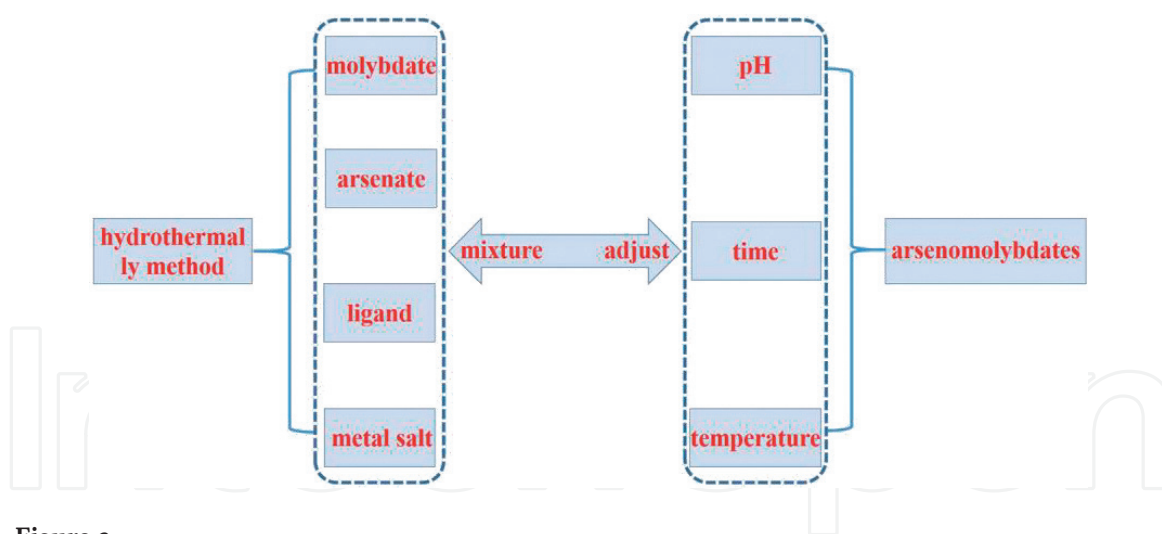


Figure 2.
 The synthesis chart of arsenomolybdates crystal.

arsenomolybdates crystals. Therefore, further exploration of synthetic conditions is necessary, which can provide more experimental data for arsenomolybdates.

2.2 Structure of classical arsenomolybdates

Up to now, various structures of arsenomolybdates were reported and discussed in detail. The following types are classical arsenomolybdates clusters: (i) $\{\text{As}_2\text{Mo}_6\}$ type, Pope's group reported the first $\{\text{As}_2\text{Mo}_6\}$ cluster [28], in which the Mo_6O_6 ring is constructed from six MoO_6 octahedra connected via an edge-sharing mode, the opposing faces have two capped AsO_4 tetrahedra. Then Zubieta's group and Ma's group reported $[\text{Mo}_x\text{O}_y\text{RAsO}_3]^{n-}$ (RAsO_3 = organoarsenic acid) and $[\text{Mo}_6\text{O}_{18}(\text{O}_3\text{AsPh})_2]^{4-}$ ($\text{Ph} = \text{PhAsO}_3\text{H}_2$) clusters [29, 30]. (ii) $\{\text{As}_6\text{Mo}_6\}$ type, which is derived from the A-type Anderson anion $[(\text{Mo}_6)\text{Mo}_6\text{O}_{18}]^{10-}$, the central $\{\text{Mo}_6\}$ octahedron is coordinated with six $\{\text{MoO}_6\}$ octahedra hexagonally arranged by sharing their edges in a plane. The cyclic As_3O_6 trimers are capped on opposite faces of Anderson-type anion plane. Each As_3O_6 group consists of three AsO_3 pyramids linked in a triangular arrangement by sharing corners and bonded to the central Mo_6 octahedron and two MoO_6 octahedra via μ_3 -oxo groups. Wang and co-workers reported the compound $(\text{C}_5\text{H}_5\text{NH})_2(\text{H}_3\text{O})_2[(\text{CuO}_6)\text{Mo}_6\text{O}_{18}(\text{As}_3\text{O}_3)_2]$ [31], Zhao groups synthesized the compound $[\text{Cu}(\text{arg})_2]_2[(\text{CuO}_6)\text{Mo}_6\text{O}_{18}(\text{As}_3\text{O}_3)_2] \cdot 4\text{H}_2\text{O}$ [32]. (iii) $\{\text{AsMo}_{12}\}$ type, has a AsO_4 tetrahedron at the center and 12 surrounding MoO_6 octahedra, such as $[\text{NBu}_4]_6[\text{Fe}(\text{C}_5\text{H}_5)_2][\text{HAsMo}_{12}\text{O}_{40}]_2$ [33]. $\{\text{As}_2\text{Mo}_9\}$ type, is derived from the trivacant Keggin moiety, which is capped by a triangular pyramidal $\{\text{AsO}_3\}$ group, e.g., $[\text{Cu}(\text{en})_2\text{H}_2\text{O}]_2\{[\text{Cu}(\text{en})_2][\text{Cu}(\text{en})_2\text{As}^{\text{III}}\text{As}^{\text{V}}\text{Mo}_9\text{O}_{34}]\} \cdot 2 \cdot 4\text{H}_2\text{O}$ and $[\text{Cu}(\text{en})_2(\text{H}_2\text{O})]_4[\text{Cu}(\text{en})_2(\text{H}_2\text{O})_2]\{[\text{Cu}(\text{phen})(\text{en})][\text{As}^{\text{III}}\text{As}^{\text{V}}\text{Mo}^{\text{VI}}_9\text{O}_{34}]_2\}$ [34, 35]. (iv) $\{\text{As}_2\text{Mo}_{18}\}$ type, as a classical Wells–Dawson cluster, can be described as two $[\text{AsMo}_9\text{O}_{34}]^{9-}$ units derived from an Keggin anion by the removal of a set of three corner-sharing MoO_6 octahedra, e.g., $[\text{Himi}]_6[\text{As}_2\text{Mo}_{18}\text{O}_{62}] \cdot 11\text{H}_2\text{O}$ [36].

In comparison with the classical arsenomolybdates, many nonclassical arsenomolybdates have also been prepared in the past of years, such as $\text{Ag}_{12.4}\text{Na}_{1.6}\text{Mo}_{18}\text{As}_4\text{O}_{71}$ [37], $(\text{NH}_4)_{11}[\text{AgAs}_2\text{Mo}_{15}\text{O}_{54}]_3 \cdot 6\text{H}_2\text{O} \cdot 2\text{CH}_3\text{CN}$ [38], $[\text{As}^{\text{III}}_2\text{Fe}^{\text{III}}_5\text{MMo}_{22}\text{O}_{85}(\text{H}_2\text{O})]^{n-}$ ($\text{M} = \text{Fe}^{3+}$, $n = 14$; $\text{M} = \text{Ni}^{2+}$ and Mn^{2+} , $n = 15$) [39], $\{\text{Cu}(2,2'\text{-bpy})\}_2\{\text{H}_2\text{As}_2\text{Mo}_2\text{O}_{14}\}$ [40], $[\{\text{Cu}(\text{imi})_2\}_3\text{As}_3\text{Mo}_3\text{O}_{15}] \cdot \text{H}_2\text{O}$ [41], and so on. The novel arsenomolybdate structure is gaining more and more attention.

3. Photocatalytic activity of arsenomolybdates

3.1 Photodegradation process

In recent years, POMs have attracted a lot of attention as photocatalysts for the decomposition of wastewater [42]. Organic dyes, such as methylene blue (MB), rhodamine B (RhB), azon phloxine (AP), and so on, is a typical organic pollutant in waste water. In this work, the photocatalytic activities of arsenomolybdates are investigated via the photodecomposition of organic dyes under UV light irradiation (**Figure 3**). The photocatalytic reactions were conducted using a common process [27]: arsenomolybdates and organic dyes solution were mixed and dispersed by ultrasonic. The suspension was stirred until reached the surface-adsorption equilibrium. Then, a high pressure Hg lamp was used as light source to irradiate the mixture, which was till stirred for keeping the mixture in suspension. At regular intervals, the sample was withdrawn from the vessel and arsenomolybdates was removed by several centrifugations, and the clear liquid was analyzed by using UV-Vis spectrophotometer.

3.2 Photocatalytic degradation of MB

The common arsenomolybdates photocatalysis are shown in **Figure 4**. The photocatalytic activities of arsenomolybdates are review via the photodecomposition of MB under UV light irradiation (**Figure 5**). Su groups reported six compounds with $[H_xAs_2Mo_6O_{26}]^{(6-x)-}$ clusters and copper-organic complexes. Six $\{As_2Mo_6\}$ compounds were irradiated for 135 min under, the photocatalytic decomposition rates are 94.5%, 93.0%, 92.1%, 92.2%, 93.6%, and 96.5%, respectively [43]. Then the $\{Co(btb)(H_2O)_2\}_2\{H_2As_2Mo_6O_{26}\} \cdot 2H_2O$ exhibited better photocatalytic activity in the degradation of MB at the same process, the photocatalytic decomposition rate is 94.27% [44]. Su groups synthesized two $\{As_2Mo_6\}$ compounds with $[H_xAs_2Mo_6O_{26}]^{(6-x)-}$ clusters and free organic ligands, photocatalytic activities of they are detected, the conversion rate of MB is 91.8% and 92.2% when adding two $\{As_2Mo_6\}$ compounds as the catalyst 160 min later, respectively [45].

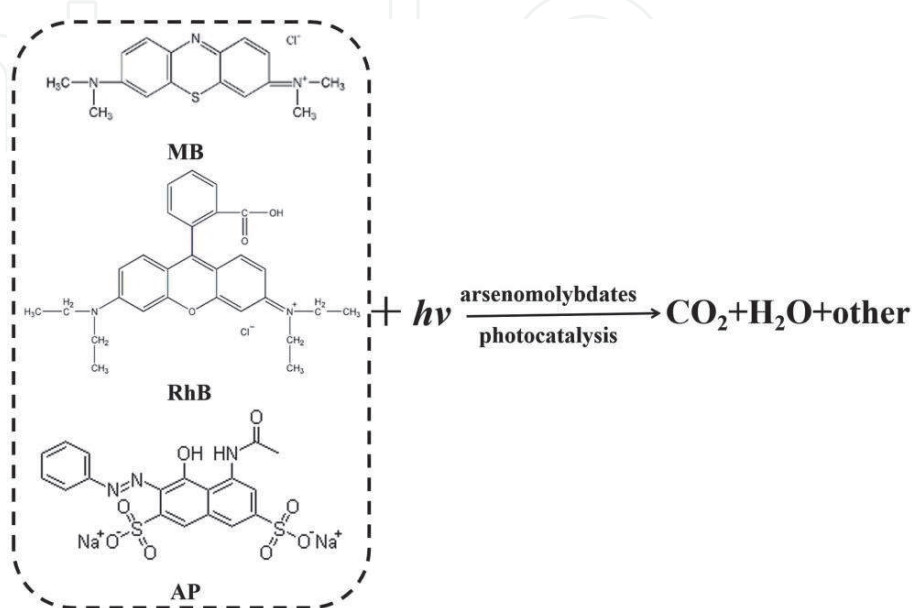


Figure 3.
The structure of dyes and photodecomposed product.

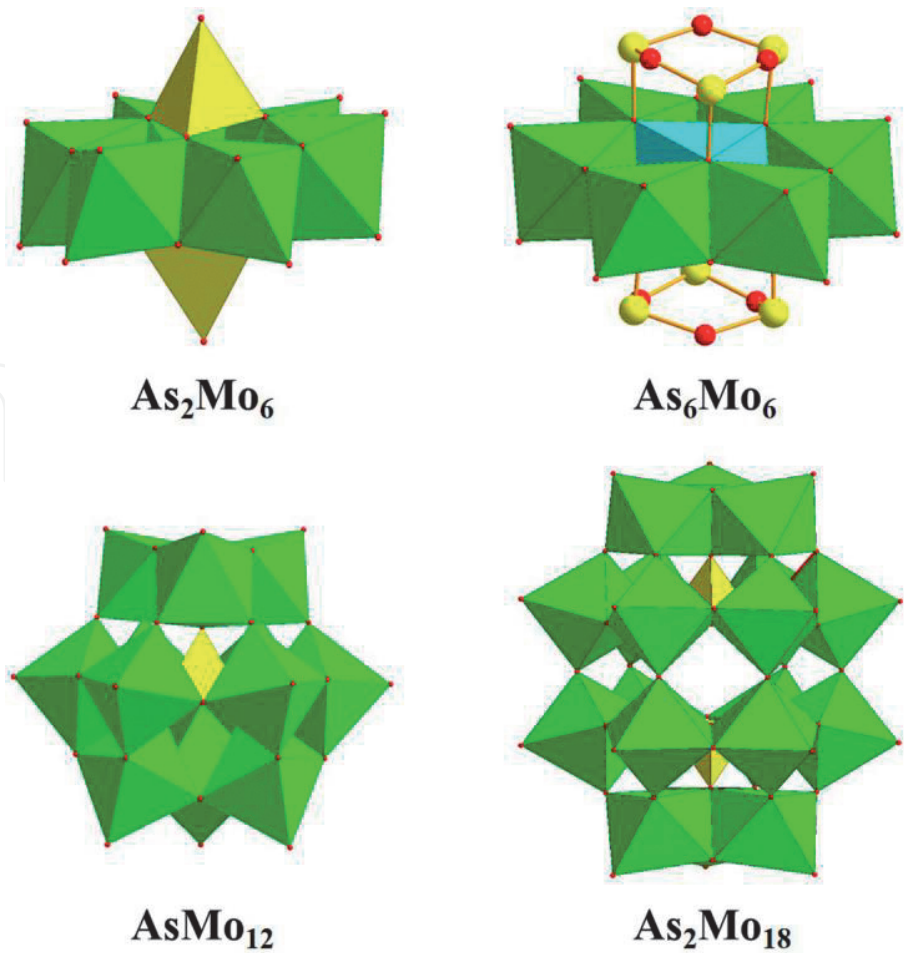


Figure 4.
The common arsenomolybdates photocatalysis polyoxoanion.

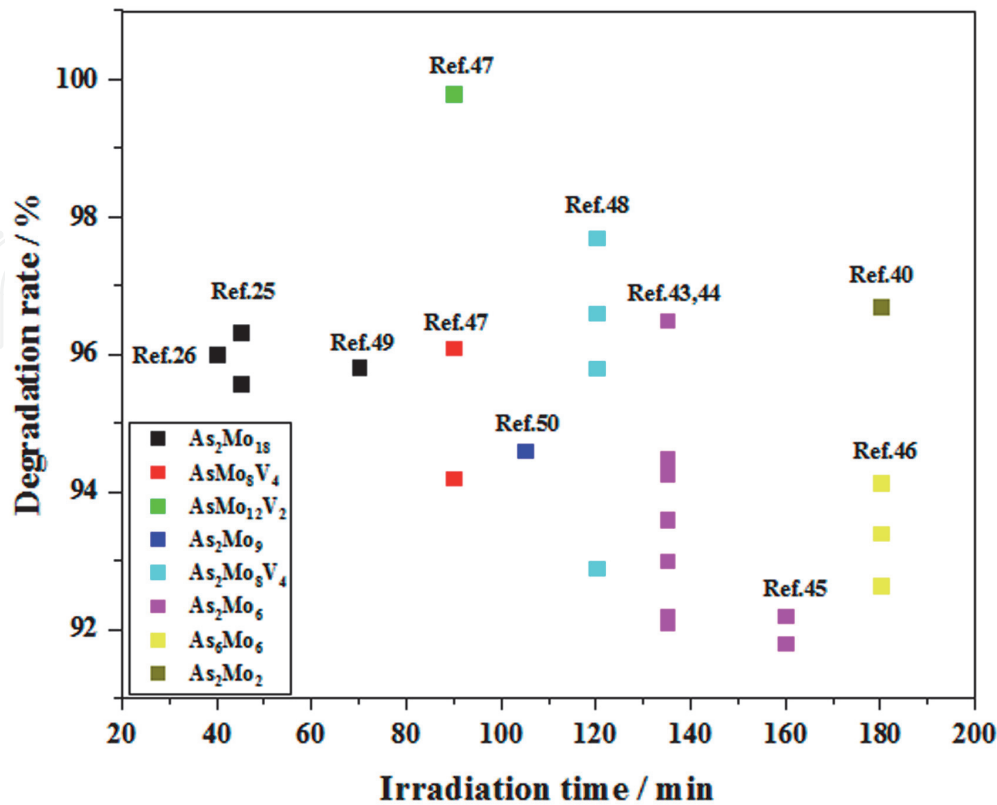


Figure 5.
The arsenomolybdates photocatalytic decomposition rates of MB under UV irradiation.

The above data show that the photocatalytic activity of the compound composed of $[H_xAs_2Mo_6O_{26}]^{(6-x)-}$ clusters and metal-organic complexes is higher than supramolecular assemblies based on isomers $[H_xAs_2Mo_6O_{26}]^{(6-x)-}$ clusters in the degradation of MB under UV irradiation, which maybe that the polyoxoanions can connect with transition metals in diverse modes, which enhanced the contact area between catalysts and substrates availing charge-transfer.

The three $\{As_6Mo_6\}$ compounds, $((phen)(H_2O)_4)_2[(CoO_6)(As_3O_3)_2Mo_6O_{18}] \cdot 2H_2O$, $\{[Co(phen)_2(H_2O)]_2[(CoO_6)(As_3O_3)_2Mo_6O_{18}]\} \cdot 4H_2O$ and $\{[Zn(biim)_2(H_2O)]_2[(ZnO_6)(As_3O_3)_2Mo_6O_{18}]\} \cdot 4H_2O$, as catalysts under UV light irradiation after 180 min [46], the photocatalytic decomposition rates of MB are about 92.64, 93.40, and 94.13%.

Yu groups prepared three Keggin arsenomolybdates, the photocatalytic decomposition rates of MB are 94.2% for $(Hbimb)(H_2bimb)[AsMo_8^{VI}V^V_4Co_2O_{40}]$, 96.1% for $(Hbimb)_2(H_2bimb)_{0.5}[AsMo_8^{VI}V^V_4Cu_2O_{40}] \cdot 1.5H_2O$, 99.8% for $[Cu^I(imi)_2][\{Cu^I(imi)_2\}_4\{AsMo_6^VMo_6^{VI}O_{40}(V^{IV}_2O_2)\}]$ after 90 min irradiation, respectively [47].

Four biarsenate(III) capped Keggin arsenomolybdates with tetravanadium(IV) substituted were prepared, which exhibit excellent degradation activity for MB under UV light. The absorption peaks of MB reduced obviously after 120 min in the presence of four Keggin arsenomolybdates, the degradation rates for MB are 92.9%, 95.8%, 96.6%, and 97.7%, respectively [48].

The photocatalytic decomposition rate of MB is about 96% for $\{[Cu(btp)_2]_3[As_2Mo_{18}O_{62}]$ after 40 min [26], and the photocatalytic decomposition rates were 96.32% and 95.57% for $[Cu(pyr)_2]_6[As_2Mo_{18}O_{62}]$ and $[Ag(pyr)_2]_6[As_2Mo_{18}O_{62}]$ after irradiation for 45 min [25]. Yu reported that $(H_2bimyb)_3(As_2Mo_{18}O_{62})$ exhibits high-efficient degradation ability for MB under UV light. After UV light irradiation of $(H_2bimyb)_3(As_2Mo_{18}O_{62})$ for 70 min, the photocatalytic decomposition rate is 95.82% [49].

It is reported that the conversion rate of MB is 94.6% when adding compound $[Cu(imi)_2]_5Na[(AsO_4)Mo_9O_{27}(AsO_3)] \cdot 5H_2O$ as the photocatalyst after 105 min [50]. $\{Cu(2,2'-bpy)\}_2[H_2As_2Mo_2O_{14}]$ as photocatalyst was investigated via the photodecomposition of MB under UV light irradiation and the same conditions. The photocatalytic decomposition rate of MB that is 96.7% after 180 min [40].

3.3 Photocatalytic degradation of RhB

The photocatalytic activities of arsenomolybdates as photocatalysts are review via the photodecomposition of RhB under UV light irradiation. The photocatalytic decomposition rates of RhB are about 96.34 and 95.7% for $\{Co(btb)(H_2O)_2\}_2[H_2As_2Mo_6O_{26}] \cdot 2H_2O$ and $\{[Cu(abi)\{H_4As^{III}As^VMo_9O_{34}\}](abi)_4[Cu(abi)_2] \cdot H_2O$ as photocatalysts under UV light irradiation after 135 and 140 min, respectively [27, 44]. $\{[Cu(btp)_2]_3[As_2Mo_{18}O_{62}]$ as photocatalyst was investigated decomposition rate of RhB after 40 min is about 96% [26]. The photocatalytic decomposition rates of RhB are 94.42 and 95.07% for $[M(pyr)_2]_6[As_2Mo_{18}O_{62}]$ ($M = Cu, Ag$) under UV light irradiation after 45 min [25].

The photocatalytic decomposition rates of RhB are 95.9% for $(Hbimb)(H_2bimb)[AsMo_8^{VI}V^V_4Co_2O_{40}]$, 94.3% for $(Hbimb)_2(H_2bimb)_{0.5}[AsMo_8^{VI}V^V_4Cu_2O_{40}] \cdot 1.5H_2O$, 95.8% for $[Cu^I(imi)_2][\{Cu^I(imi)_2\}_4\{AsMo_6^VMo_6^{VI}O_{40}(V^{IV}_2O_2)\}]$ after 108 min irradiation, respectively [47].

3.4 Photocatalytic degradation of AP

AP, as one of the azo dyes, is relatively difficult to degrade, and so it was used as target molecules to evaluate the photocatalytic activity of arsenomolybdates under

UV irradiation. The photocatalytic activity of $\{\text{pyr}\}\{\text{Hbib}\}_2\{\text{As}^{\text{III}}_2(\text{OH})_2\text{As}^{\text{V}}_2\text{Mo}_{18}\text{O}_{62}\}$ was evaluated for the degradation of AP under UV irradiation [51], the degradation rate is 91.02% after UV light irradiation 90 min. In addition, the photocatalytic activity of noncapped 0D analog $(\text{H}_2\text{bimy})_3(\text{As}_2\text{Mo}_{18}\text{O}_{62})$ was also studied under the same condition. Compared with $\{\text{pyr}\}\{\text{Hbib}\}_2\{\text{As}^{\text{III}}_2(\text{OH})_2\text{As}^{\text{V}}_2\text{Mo}_{18}\text{O}_{62}\}$, only 32.76% of AP was degraded by $(\text{H}_2\text{bimy})_3(\text{As}_2\text{Mo}_{18}\text{O}_{62})$ after 90 min [49], which indicates that the photocatalytic degradation effect of the bi-arsenic capped Dawson compound on AP is much better than that of noncapped analog. The 3D Dawson organic-inorganic hybrid arsenomolybdate, $\{\text{Ag}(\text{diz})_2\}_3[\{\text{Ag}(\text{diz})_2\}_3(\text{As}_2\text{Mo}_{18}\text{O}_{62})] \cdot \text{H}_2\text{O}$ exhibits merit photocatalytic properties for degradation of refractory dyes AP under UV light [52], the photocatalytic decomposition rate is 93.24% after 80 min.

The photocatalytic activities of $(\text{imi})_2[\{\text{Cu}^{\text{I}}(\text{imi})_2\}_2\{\text{Na}(\text{imi})_2\}\{\text{As}^{\text{III}}\text{As}^{\text{V}}\text{Mo}_{18}\text{O}_{62}\}] \cdot 2\text{H}_2\text{O}$ and $\{\text{Cu}^{\text{I}}_{0.5}(\text{trz})\}_6[\{\text{Cu}^{\text{I}}_{0.5}(\text{trz})\}_6(\text{As}_2\text{Mo}_{18}\text{O}_{62})]$ were evaluated for degradation of AP under UV irradiation. The photocatalytic decomposition rates are 89.06 and 96.38% after 80 min [53]. The photocatalytic decomposition rates are 92.49% of AP for $[\text{Cu}(\text{pyr})_2]_6[\text{As}_2\text{Mo}_{18}\text{O}_{62}]$ and 92.25% of AP for $[\text{Ag}(\text{pyr})_2]_6[\text{As}_2\text{Mo}_{18}\text{O}_{62}]$ after irradiation 135 min [25].

On the basis of the aforementioned points, $\{\text{As}_2\text{Mo}_{18}\}$ type arsenomolybdates with 3D networks possess the highest photocatalytic activities for photodecomposition of MB, RhB and AP under UV light irradiation. The following factors are maybe considered: First, quantity of Mo and O atoms in unit cell is a factor, which can increases the amount of charge-transfer from HOMO of O to LUMO of Mo, generating more electron-hole pairs. Second, the enhanced photocatalytic activity may have arisen from the 3D architecture, more extended 3D frameworks favor the migration of excited holes/electrons to the surfaces of $\{\text{As}_2\text{Mo}_{18}\}$ type to initiate the photocatalytic degradation reaction with organic dyes.

3.5 Reaction mechanisms of photocatalytic performance

Experimental and theoretical studies of arsenomolybdates photocatalysis have revealed that it typically proceeds based on the following mechanism [41, 42, 48, 52]: Irradiated of arsenomolybdates by UV light with energy equal to or greater than the E_g value of itself, which induces intramolecular charge-transfer from the HOMO of O to the LUMO of Mo, leading to the formation of photoexcited states, subsequently photogenerated electron-hole pairs were generated. The O_2 captures electron to form $\cdot\text{O}_2^-$ and the hole reacts with H_2O or OH^- ions to form $\cdot\text{OH}$. The $\cdot\text{O}_2^-$ and $\cdot\text{OH}$ radical decompose organic dyes' molecules into the final product, the detail of photocatalytic reaction is shown in Eqs. (1)–(4).



3.6 Stability

Some research data show that the samples were washed and dried after the arsenomolybdates as photocatalysis several cycles, and the infrared or X-ray diffraction test were carried out, the infrared spectra or X-ray diffraction data of arsenomolybdates demonstrate that there are almost unchanged before and after

photocatalytic reaction [44–48], which indicate that arsenomolybdates photocatalysis have excellent structural stability.

4. Conclusions

In this chapter, the arsenomolybdates are presented, and the attention is mainly focus on photocatalytic degradation of organic dyes. Various strategies are summarized and discussed based on the knowledge of synthesis, structure and photocatalytic properties for arsenomolybdates, which reflects the major directions of recent research in this field. There are vast research opportunities as new arsenomolybdates architectures are discovered in future; the great effort to promote the development of arsenomolybdates is needed to reduce the gap with commercial applications.

Acknowledgements

This work was supported by the Project of Introducing Talent of Guangdong University of Petrochemical Technology (2019rc052).

Conflict of interest

The authors declare no competing financial interest.

Abbreviations

arg	L-arginine
en	ethylenediamine
imi	imidazole
2,2'-bipy	2,2'-bipyridine
btb	1,4-bis(1,2,4-triazol-1-yl)butane)
phen	1,10'-phenanthroline
biim	biimidazole
bimb	1,4-Bis(imidazol-1-yl)butane
btp	1,3-bis(1,2,4-triazol-1-yl)propane
pyr	pyrazole
bib	1, 4-bis(1-imidazolyl)benzene
bimyb	1,4-Bis(imidazol-1-ylmethyl) benze
abi	2-aminobenzimidazole
bib	1,4-bis(1-imidazolyl)benzene
diz	1,2-diazole
trz	1,2,3-triazole

IntechOpen

IntechOpen

Author details

Zhi-Feng Zhao
College of Chemistry, Guangdong University of Petrochemical Technology,
Maoming, China

*Address all correspondence to: zhifengzhao1980@163.com

IntechOpen

© 2020 The Author(s). Licensee IntechOpen. This chapter is distributed under the terms of the Creative Commons Attribution License (<http://creativecommons.org/licenses/by/3.0>), which permits unrestricted use, distribution, and reproduction in any medium, provided the original work is properly cited. 

References

- [1] Sha JQ, Zhu PP, Yang XY, Li XN, Li X, Yue MB, et al. Polyoxometalates templated metal Ag–carbene frameworks anodic material for lithium-ion batteries. *Inorganic Chemistry*. 2017;**56**:11998-12002. DOI: 10.1021/acs.inorgchem.7b01962
- [2] Armatas NG, Ouellette W, Whitenack K, Pelcher J, Liu HX, Romaine E, et al. Construction of metal–organic oxides from molybdophosphonate clusters and copper-bipyrimidine building blocks. *Inorganic Chemistry*. 2009;**48**: 8897-8910. DOI: 10.1021/ic901133k
- [3] Azambuja FD, Parac-Vogt TN. Water-tolerant and atom economical amide bond formation by metal-substituted polyoxometalate catalysts. *ACS Catalysis*. 2019;**9**:10245-10252. DOI: 10.1021/acscatal.9b03415
- [4] Long DL, Tsunashima R, Cronin L. Polyoxometalates: Building blocks for functional nanoscale systems. *Angewandte Chemie, International Edition*. 2010;**49**(10):1736-1758. DOI: 10.1002/anie.200902483
- [5] Pang HJ, Yang M, Kang L, Ma HY, Liu B, Li SB, et al. An unusual 3D interdigitated architecture assembled from Keggin polyoxometalates and dinuclear copper(II) complexes. *Journal of Solid State Chemistry*. 2013;**198**: 440-444. DOI: 10.1016/j.jssc.2012.11.007
- [6] Hagrman PJ, Hagrman D, Zubieta J. Organic–inorganic hybrid materials: From “simple” coordination polymers to organodiamine-templated molybdenum oxides. *Angewandte Chemie International Edition*. 1999;**38**(18): 2638-2684. DOI: 10.1002/(SICI)1521-3773(19990917)38:18<2638::AID-ANGE2638>3.0.CO;2-4
- [7] Kim D, Seog JH, Kim MJ, Yang MH, Gillette E, Lee SB, et al. Polyoxometalate-mediated one-pot synthesis of Pd nanocrystals with controlled morphologies for efficient chemical and electrochemical catalysis. *Chemistry–A European Journal*. 2015;**21**: 5387-5394. DOI: 10.1002/chem.201406400
- [8] Walsh JJ, Bond AM, Forster RJ, Keyes TE. Hybrid polyoxometalate materials for photo(electro-) chemical applications. *Coordination Chemistry Reviews*. 2016;**306**:217-234. DOI: 10.1016/j.ccr.2015.06.016
- [9] Wang XL, Rong X, Lin HY, Cao JJ, Liu GC, Chang ZH. A novel Wells–Dawson polyoxometalate-based metal–organic framework constructed from the uncommon in-situ transformed bi (triazole) ligand and azo anion. *Inorganic Chemistry Communications*. 2016;**63**:30-34. DOI: 10.1016/j.inoche.2015.11.004
- [10] Sha JQ, Sun LJ, Zhu PP, Jiang JZ. The first two-fold interpenetrating polyoxometalate-based coordination polymer with helical channels: Structure and catalytic activities. *CrystEngComm*. 2016;**18**:283-289. DOI: 10.1039/C5CE02021B
- [11] Zhao ZF, Ding YZ, Bi JC, Su ZH, Cai QH, Gao LM, et al. Molybdenum arsenate crystal: A highly efficient and recyclable catalyst for hydrolysis of ethylene carbonate. *Applied Catalysis A: General*. 2014;**471**:50-55. DOI: 10.1016/j.apcata.2013.11.028
- [12] Peng G, Wang YH, Hu CW, Wang EB, Feng SH, Zhou YC, et al. Heteropolyoxometalates which are included in microporous silica, $\text{Cs}_x\text{H}_{3-x}\text{PMo}_{12}\text{O}_{40}/\text{SiO}_2$ and $\text{Cs}_y\text{H}_{5-y}\text{PMo}_{10}\text{V}_2\text{O}_{40}/\text{SiO}_2$, as insoluble solid bifunctional catalysts: Synthesis and selective oxidation of benzyl alcohol in liquid–solid systems. *Applied*

- Catalysis A: General. 2001;**218**:91-99. DOI: 10.1016/S0926-860X(01)00622-6
- [13] Chalkley L. The extent of the photochemical reduction of phosphotungstic acid. *The Journal of Physical Chemistry*. 1952;**56**(9): 1084-1086. DOI: 10.1021/j150501a012
- [14] Hill CL, Bouchard DA. Catalytic photochemical dehydrogenation of organic substrates by polyoxometalates. *Journal of the American Chemical Society*. 1985;**107**:5148-5157. DOI: 10.1021/ja00304a019
- [15] Tamimi M, Heravi MM, Mirzaei M, Zadsirjan V, Lotfian N, Eshtiagh-Hosseini H. $\text{Ag}_3[\text{PMo}_{12}\text{O}_{40}]$: An efficient and green catalyst for the synthesis of highly functionalized pyran-annulated heterocycles via multicomponent reaction. *Applied Organometallic Chemistry*. 2019;**33**: e5043-e5045. DOI: 10.1002/aoc.5043
- [16] Daraie M, Heravi MM, Mirzaei M, Lotfian N. Synthesis of Pyrazolo-[4,3,6] pyrido [2,3-d] pyrimidine-diones catalyzed by a nano-sized surface-grafted neodymium complex of the tungstosilicate via multicomponent reaction. *Applied Organometallic Chemistry*. 2019;**33**:e5058. DOI: 10.1002/aoc.5058
- [17] López X, Carbó JJ, Bo C, Poblet JM. Structure, properties and reactivity of polyoxometalates: A theoretical perspective. *Chemical Society Reviews*. 2012;**41**:7537-7571. DOI: 10.1039/C2CS35168D
- [18] Proust A, Thouvenot R, Gouzerh P. Functionalization of polyoxometalates: Towards advanced applications in catalysis and materials science. *Chemical Communications*. 2008;**16**: 1837-1852. DOI: 10.1039/B715502F
- [19] Song YF, Tsunashima R. Recent advances on polyoxometalate-based molecular and composite materials. *Chemical Society Reviews*. 2012;**41**: 7384-7402. DOI: 10.1039/C2CS35143A
- [20] Proust A, Matt B, Villanneau R, Guillemot G, Gouzerh P, Izzet G. Functionalization and post-functionalization: A step towards polyoxometalate-based materials. *Chemical Society Reviews*. 2012;**41**: 7605-7622. DOI: 10.1039/C2CS35119F
- [21] Pope MT, Müller A. Polyoxometalate chemistry: An old field with new dimensions in several disciplines. *Angewandte Chemie, International Edition*. 1991;**30**:34-48. DOI: 10.1002/anie.199100341
- [22] Chen CC, Wang Q, Lei PX, Song WJ, Ma WH, Zhao JC. Photodegradation of dye pollutants catalyzed by porous $\text{K}_3\text{PW}_{12}\text{O}_{40}$ under visible irradiation. *Environmental Science & Technology*. 2006;**40**: 3965-3970. DOI: 10.1021/es060146j
- [23] Wu PF, Zhang YP, Feng CT, Liu B, Hu HM, Xue GL. A large, X-shaped polyoxometalate $[\text{As}_6\text{Fe}_7\text{Mo}_{22}\text{O}_{98}]^{25-}$ assembled from $[\text{AsMo}_7\text{O}_{27}]^{9-}$ and $[\text{FeMo}_4\text{O}_{19}]^{11-}$ moieties. *Dalton Transactions*. 2018;**47**:15661-15665. DOI: 10.1039/C8DT02647E
- [24] Zhu TT, Wang J, Chen SH. Synthesis and anti-lung cancer activity of a novel arsenomolybdate compound. *Journal of Molecular Structure*. 2017; **1149**:766-770. DOI: 10.1016/j.molstruc.2017.08.032
- [25] Cong BW, Su ZH, Zhao ZF, Yu BY, Zhao WQ, Ma XJ. Two unusual 3D honeycomb networks based on Wells-Dawson arsenomolybdates with d^{10} transition-metal-pyrazole connectors. *Dalton Transactions*. 2017;**46**:7577-7583. DOI: 10.1039/c7dt01240c
- [26] Cong BW, Su ZH, Zhao ZF, Wang B. A novel 3D POMOF based on Wells-Dawson arsenomolybdates with excellent photocatalytic and lithium-ion

- battery performance. *CrystEngComm*. 2017;**19**:7154-7161. DOI: 10.1039/c7ce01734k
- [27] Zhao ZF, Su ZH, Cong BW, Gao W, Ma XJ. The new arsenomolybdate based on monocapped trivacant Keggin $\{H_4As^{III}As^VMo_9O_{34}\}$ cluster and Cu-abi complex: Synthesis, structure, photoluminescence and catalysis properties. *Journal of Cluster Science*. 2018;**29**:943-949. DOI: 10.1007/s10876-018-1390-6
- [28] Kwak W, Rajkovic LM, Stalick JK, Pope MT, Quicksall CO. Synthesis and structure of hexamolybdobis (organoarsonates). *Inorganic Chemistry*. 1976;**15**(11):2778-2783. DOI: 10.1021/ic50165a042
- [29] Liu B, Yang J, Yang GC, Ma JF. Four new three-dimensional polyoxometalate-based metal-organic frameworks constructed from $[Mo_6O_{18}(O_3AsPh)_2]^{4-}$ polyoxoanions and copper(I)-organic fragments: Syntheses, structures, electrochemistry, and photocatalysis properties. *Inorganic Chemistry*. 2013;**52**:84-94. DOI: 10.1021/ic301257k
- [30] Burkholder E, Wright S, Golub V, O'Connor CJ, Zubieta J. Solid state coordination chemistry of oxomolybdenum organoarsenate materials. *Inorganic Chemistry*. 2003;**42**:7460-7471. DOI: 10.1021/ic030171f
- [31] He Q, Wang E. Hydrothermal synthesis and crystal structure of a new copper(II) molybdenum(VI) arsenate (III), $(C_5H_5NH)_2(H_3O)_2[(CuO_6)Mo_6O_{18}(As_3O_3)_2]$. *Inorganic Chemistry Communications*. 1999;**2**(9):399-402
- [32] Zhao JW, Zhang JL, Li YZ, Cao J, Chen LJ. Novel one-dimensional organic-inorganic polyoxometalate hybrids constructed from heteropolymolybdate units and copper-aminoacid complexes. *Crystal Growth & Design*. 2014;**14**:1467-1475. DOI: 10.1021/cg500019g
- [33] Li ZF, Cui RR, Liu B, Xue GL, Hu HM, Fu F, et al. Structural and property characterization of two new charge-transfer salts based on Keggin ions and ferrocene. *Journal of Molecular Structure*. 2009;**920**:436-440. DOI: 10.1016/j.molstruc.2008.12.004
- [34] Han QX, Ma PT, Zhao JW, Wang ZL, Yang WH, Guo PH, et al. Three novel inorganic-organic hybrid Arsenomolybdate architectures constructed from Monocapped Trivacant $[As^{III}As^VMo_9O_{34}]^{6-}$ fragments with $[Cu(L)_2]^{2+}$ linkers: From dimer to two-dimensional framework. *Crystal Growth & Design*. 2011;**11**(2): 436-444. DOI: 10.1021/cg101125m
- [35] Niu JY, Hua JA, Ma X, Wang JP. Temperature-controlled assembly of a series of inorganic-organic hybrid arsenomolybdates. *CrystEngComm*. 2012;**14**:4060-4067. DOI: 10.1039/C2CE00030J
- [36] Yang YY, Xu L, Jia LP, Gao GG, Li FY, Qu XS, et al. Crystal structure and electrochemical properties of the supramolecular compound $[Himi]_6[As_2Mo_{18}O_{62}] \cdot 11H_2O$. *Crystal Research and Technology*. 2007;**42**(10): 1036-1040. DOI: 10.1002/crat.200710937
- [37] Hajji M, Zid MF. Synthesis, structure and ionic conductivity of the molybdenum arsenate: $Ag_{12.4}Na_{1.6}Mo_{18}As_4O_{71}$. *Solid State Sciences*. 2012;**14**(9):1349-1354. DOI: 10.1016/j.solidstatesciences.2012.07.021
- [38] Zhang YP, Li LL, Sun T, Hu HM, Xue GL. A cage-like polyanion with a Ag + enwrapped, $[AgAs_2Mo_{15}O_{54}]^{11-}$. *Inorganic Chemistry*. 2011;**50**: 2613-2618. DOI: 10.1021/ic102459r
- [39] Liu B, Li LL, Zhang YP, Ma Y, Hu HM, Xue GL. Three banana-shaped

arsenomolybdates encapsulating a hexanuclear transition-metal central magnetic cluster: $[\text{As}^{\text{III}}_2\text{Fe}^{\text{III}}_5\text{MMo}_{22}\text{O}_{85}(\text{H}_2\text{O})]^{n-}$ ($\text{M} = \text{Fe}^{3+}$, $n = 14$; $\text{M} = \text{Ni}^{2+}$ and Mn^{2+} , $n = 15$). *Inorganic Chemistry*. 2011;**50**:9172-9177. DOI: 10.1021/ic201418q

[40] Zhao WQ, Su ZH, Zhao ZF, Cong BW, Xia L, Zhou BB. The synthesis, structure and properties of a new compound with 1D linear chain arsenomolybdate anion building block. *Inorganic Chemistry Communications*. 2015;**61**:118-122. DOI: 10.1016/j.inoche.2015.09.008

[41] Zhao ZF, Zhou BB, Su ZH, Ma HY, Li CX. A new $[\text{As}_3\text{Mo}_3\text{O}_{15}]^{3-}$ fragment decorated with Cu(I)-Imi (Imi = imidazole) complexes: Synthesis, structure and electrochemical properties. *Inorganic Chemistry Communications*. 2008;**11**:648-651. DOI: 10.1016/j.inoche.2008.02.032

[42] Patel A, Patel K. Cs salt of di-manganese(II) substituted phosphotungstate: One pot synthesis, structural, spectroscopic characterization and solvent free liquid phase oxidation of styrene using different oxidants. *Polyhedron*. 2014;**69**:110-118. DOI: 10.1016/j.poly.2013.11.033

[43] Cong BW, Su ZH, Zhao ZF, Yu BY, Zhao WQ, Xia L, et al. Assembly of six $[\text{H}_x\text{As}_2\text{Mo}_6\text{O}_{26}]^{(6-x)-}$ cluster-based hybrid materials from 1D chains to 3D framework with multiple Cu-N complexes. *CrystEngComm*. 2017;**19**:2739-2749. DOI: 10.1039/c7ce00319f

[44] Cong BW, Su ZH, Zhao ZF, Zhao WQ, Ma XJ, Zhou BB. A new rhombic 2D interpenetrated organic-inorganic hybrid material base on $[\text{H}_x\text{As}_2\text{Mo}_6\text{O}_{26}]^{(6-x)-}$ polyoxoanion and Co-btb complexes. *Inorganic Chemistry Communications*. 2017;**83**:11-15. DOI: 10.1016/j.inoche.2017.05.024

[45] Zhao ZF, Su ZH, Cong BW, Zhao WQ, Ma XJ. Organic-inorganic hybrid supramolecular assemblies based on isomers $[\text{H}_x\text{As}_2\text{Mo}_6\text{O}_{26}]^{(6-x)-}$ clusters. *Zeitschrift für Anorganische und Allgemeine Chemie*. 2017;**643**:980-984. DOI: 10.1002/zaac.201700157

[46] Cong BW, Su ZH, Zhao ZF, Zhao WQ, Xia L, Zhou BB. The pH-controlled assembly of a series of inorganic-organic hybrid arsenomolybdates based on $[(\text{Mo}_6)(\text{As}_3\text{O}_3)_2\text{Mo}_6\text{O}_{18}]^{4-}$ cluster. *Polyhedron*. 2017;**127**:489-495. DOI: 10.1016/j.poly.2016.10035

[47] Li FR, Lv JH, Yu K, Zhang ML, Wang KP, Meng FX, et al. Effective photocatalytic and bifunctional electrocatalytic materials based on Keggin arsenomolybdate and different transition metal capped assemblies. *CrystEngComm*. 2018;**20**:3522-3534. DOI: 10.1039/C8CE00550H

[48] Zhao ZF, Cong BW, Su ZH, Li BR. Self-assembly of biarsenate capped Keggin arsenomolybdates with tetravanadium-substituted for photocatalytic degradation of organic dyes. *Crystal Growth & Design*. 2020;**20**:2753-2760. DOI: 10.1021/acs.cgd.0c00123

[49] Cai HH, Lü JH, Yu K, Zhang H, Wang CM, Wang L, et al. Organic-inorganic hybrid supramolecular assembly through the highest connectivity of a Wells-Dawson molybdoarsenate. *Inorganic Chemistry Communications*. 2015;**62**:24-28. DOI: 10.1016/j.inoche.2015.10.006

[50] Zhao ZF, Su ZH, Zhao WQ, Gao W, Cong BW, Zhou BB. The hybrid organic-inorganic assemblies based on monocapped trivacant Keggin arsenatomolybdate and CuI-organic units. *Journal of Cluster Science*. 2016;**27**:1579-1590. DOI: 10.1007/s10876-016-1022-y

[51] Lv PJ, Yuan J, Yu K, Shen JH. An unusual bi-arsenic capped Well-Dawson arsenomolybdate hybrid supramolecular material with photocatalytic property and anticancer activity. *Journal of Inorganic and Organometallic Polymers and Materials*. 2018;**28**:899-905. DOI: 10.1007/s10904-017-0760-0

[52] Lv PJ, Cao WW, Yu K, Shen JH. A novel 2, 6-connected inorganic-organic 3-D open framework based on $\{\text{As}_2\text{Mo}_{18}\}$ with photocatalytic property and anticancer activity. *Inorganic Chemistry Communications*. 2017;**79**: 95-98. DOI: 10.1016/j.inoche.2017.03.028

[53] Li FR, Lv JH, Yu K, Zhang H, Wang CM, Wang CX, et al. Two extended Wells–Dawson arsenomolybdate architectures directed by Na(I) and/or Cu(I) organic complex linkers. *CrystEngComm*. 2017;**19**: 2320-2328. DOI: 10.1039/C6CE02539K